SLAC–PUB–6638
August 1994
(T/E)

EXPERIMENTAL RESULTS ON POLARIZED STRUCTURE FUNCTIONS IN DEEP INELASTIC LEPTON-NUCLEON SCATTERING*

LINDA STUART†

Stanford Linear Accelerator Center

Stanford University, Stanford, California 94309

Abstract

A summary is given of experimental results on spin structure functions of the proton $g_1^p(x,Q^2)$, deuteron $g_1^d(x,Q^2)$, and neutron $g_1^n(x,Q^2)$ as measured in deep inelastic scattering of polarized leptons from a polarized target. All results are consistent with the Bjorken sum rule predictions at the Q^2 of each experiment. The data do not support the Ellis-Jaffe sum rule prediction for the proton which implies that the helicity carried by the strange quark may be nonzero and that the net quark helicity is smaller than expected from simple quark models.

Presented at the Tennessee International Symposium on Radiative Corrections

Gatlinburg, Tennessee, June 27–July 1, 1994

*Work supported by Department of Energy contract DE–AC03–76SF00515.
†Representing the E142 and E143 Collaborations.

1. Introduction

Measurements of the spin-dependent structure functions $g_1(x,Q^2)$ for the proton, deuteron, and neutron are valuable tools used to understand the complex nature of nucleon spin structure. The structure functions are used for testing sum rules and in the quark model can be used to determine the fraction of the nucleon helicity carried by constituent quarks.

The spin-dependent structure functions $g_1(x,Q^2)$ and $g_2(x,Q^2)$ are extracted from measured deep inelastic cross-section asymmetries. The longitudinal and transverse asymmetries are defined as

$$\begin{aligned} A_\parallel &= \frac{\sigma^{\downarrow\uparrow}-\sigma^{\uparrow\uparrow}}{\sigma^{\downarrow\uparrow}+\sigma^{\uparrow\uparrow}} = f\Big[g_1(x,Q^2)[E+E'\cos(\theta)] - \frac{Q^2}{\nu}g_2(x,Q^2)\Big] \\ A_\perp &= \frac{\sigma^{\downarrow\leftarrow}-\sigma^{\uparrow\leftarrow}}{\sigma^{\downarrow\leftarrow}+\sigma^{\uparrow\leftarrow}} = fE'\sin(\theta)\Big[g_1(x,Q^2)+\frac{2E}{\nu}g_2(x,Q^2)\Big], \end{aligned} \tag{1}$$

where $\sigma^{\uparrow\uparrow}(\sigma^{\downarrow\uparrow})$ corresponds to the measured inclusive cross section for parallel (antiparallel) beam and target longitudinal polarizations; $\sigma^{\uparrow\leftarrow}(\sigma^{\downarrow\leftarrow})$ is similar, except the target polarization is transverse; E and E' are the incident and scattered lepton energies, θ is the scattering angle, Q^2 is the four-momentum transfer squared, $\nu = E-E'$, $x = Q^2/2M\nu$, and M is the mass of the nucleon. The factor f is defined by the unpolarized structure functions, $F_2(x,Q^2)$ and $F_1(x,Q^2) = F_2(x,Q^2)(1+\gamma^2)/(2x(1+R(x,Q^2)))$

$$f = \frac{1}{F_1(x,Q^2)}\ \frac{1}{\nu}\ \frac{1-\epsilon}{1+\epsilon R(x,Q^2)}\ , \tag{2}$$

where $R(x,Q^2) = \sigma_L/\sigma_T$ is the ratio of longitudinal and transverse virtual photoabsorption cross-sections, $\epsilon = 1/[1+2(1+\nu^2/Q^2)\tan^2(\theta/2)]$ is the longitudinal virtual photon polarization, and $\gamma^2 = Q^2/\nu^2$. Also of interest are the virtual photon absorption asymmetries

$$\begin{aligned} A_1 &= \frac{\sigma_{1/2}-\sigma_{3/2}}{\sigma_{1/2}+\sigma_{3/2}} = (g_1(x,Q^2)-\gamma^2 g_2(x,Q^2))/F_1(x,Q^2) \\ A_2 &= \frac{2\sigma_{TL}}{\sigma_{1/2}+\sigma_{3/2}} = \gamma(g_1(x,Q^2)+g_2(x,Q^2))/F_1(x,Q^2)\ , \end{aligned} \tag{3}$$

where $\sigma_{1/2}$ and $\sigma_{3/2}$ are the helicity conserving and nonconserving virtual photon-nucleon absorption cross sections, and σ_{TL} is an interference term between the transverse and longitudinal photon-nucleon amplitudes. Equations (1) to (3) can be combined to give

$$g_1(x,Q^2) = \frac{1}{f(E+E')}\,[A_\parallel + \tan(\theta/2)A_\perp] = \frac{F_1}{1+\gamma^2}\,(A_1+\gamma A_2)\ . \tag{4}$$

In the limit that θ is small and γ is small, Eq. (4) reduces to the often-used expressions

$$\frac{g_1(x,Q^2)}{F_1(x,Q^2)} \simeq \frac{A_\parallel}{fF_1(x,Q^2)(E+E')} \simeq \frac{A_\parallel}{D} \simeq A_1 \ , \tag{5}$$

where $D = (1 - E'\epsilon/E)/(1 + \epsilon R(x,Q^2)$ is the virtual photon depolarization factor.

1.1. Sum Rules

A sum rule originally developed by Bjorken [1] relates the integral over the difference between the proton and neutron spin structure functions to the nucleon beta decay weak coupling constants. It is believed to be strictly valid at infinite Q^2:

$$\int_0^1 (g_1^p(x) - g_1^n(x))\,dx = \frac{1}{6}\frac{g_A}{g_V} \qquad \text{for} \quad Q^2 = \infty \ , \tag{6}$$

where g_A and g_V are the nucleon axial-vector and vector coupling constants and $g_A/g_V = 1.2573 \pm 0.0038$ [2]. The advent of QCD corrections has brought this sum rule into the regime where it, and thus the QCD corrections, can be experimentally tested. These nonsinglet corrections to order three for three quark flavors are [3]

$$C_{NS} = \left[1 - \frac{\alpha_s(Q^2)}{\pi} - 3.58\left(\frac{\alpha_s(Q^2)}{\pi}\right)^2 - 20.22\left(\frac{\alpha_s(Q^2)}{\pi}\right)^3\right] \ , \tag{7}$$

where $\alpha_s(Q^2)$ is the strong coupling constant.

Other sum rules of interest, although less rigorous, are the Ellis-Jaffe sum rules [4] which were derived using SU(3) symmetry and assuming the strange sea in the nucleons is unpolarized. Including second order QCD singlet corrections [5], C_S, they are expressed:

$$\begin{aligned}
\Gamma_1^p(Q^2) &= \int_0^1 g_1^p(x,Q^2)\,dx = \frac{1}{18}\,[C_{NS}(3F+D) + 2C_S(3F-D)] \\
\Gamma_1^n(Q^2) &= \int_0^1 g_1^n(x,Q^2)\,dx = \frac{1}{9}\,[-DC_{NS} + C_S(3F-D)] \ ,
\end{aligned} \tag{8}$$

where F and D are weak hyperon decay constants and can be extracted from the data [6] $F/D = 0.575 \pm 0.016$ and $F + D = g_A/g_V$.

1.2. Quark Model Interpretation

In the quark model, the spin-dependent structure function $g_1(x)$ is interpreted as the charge-weighted difference between momentum distributions for quarks with helicities aligned parallel ($\uparrow$) and antiparallel ($\downarrow$) to that of the nucleon:

$$g_1(x) = \frac{1}{2}\sum_i e_i^2\,[q_i^\uparrow(x) - q_i^\downarrow(x)] \equiv \sum_i e_i^2 \Delta q_i(x), \tag{9}$$

where e_i is the charge of quark species i, and $q_i^{\uparrow(\downarrow)}(x)$ are the quark plus antiquark momentum distributions. The quantity $\int_0^1 \Delta q_i(x)dx = \Delta i$ refers to the helicity of quark species $i = u, d, s$ in the proton, and $\Delta q = \Delta u + \Delta d + \Delta s$ is the net helicity of quarks. Using measurements of $\int_0^1 g_1(x)dx$, g_A/g_V, and F/D, as well as the QCD corrections to the sum rules, the quantities Δ_i can be separately extracted.

2. Early SLAC and EMC Experiments

The earliest spin structure experiments, E80 [7], E130 [8], and EMC [9] measured $A_\parallel$ for the proton only. In order to extract information on the structure function $g_1^p(x,Q^2)$, it was necessary to make assumptions as indicated in Eq. (5). The SLAC [7,8] data are statistics limited and only cover an x range greater than 0.1. It was not until EMC [9] measured $g_1^p(x,Q^2)$ with higher precision down to an x of 0.015 that the so-called "spin crisis" was born. These results indicated that the proton Ellis-Jaffe sum rule was violated. The EMC reported a measured value of $\Gamma_p = 0.126 \pm 0.018$ at $Q^2 = 10.7$ (GeV/c)^2, while the sum rule predicted $\Gamma_p = 0.175 \pm 0.007$ at the same Q^2. In addition, the extracted quark helicities were $\Delta q = 0.12 \pm 0.17$ and $\Delta s = -0.19 \pm 0.06$. The total quark helicity was small and consistent with zero, while the strange quark helicity was negative and inconsistent with zero. This unexpected result has generated a lot of interest in the physics community. Many theoretical papers have surfaced to explain the data, better QCD corrections have been calculated which bring the predictions closer to experimental results, and extensive experimental programs at SLAC, CERN, and HERA were begun to learn more about the proton spin structure, and to make the first measurements of the neutron spin structure. Although it is generally believed that there is no "crisis" today, the impact on both theoretical and experimental spin structure physics has been great, and has thus served to further our understanding of nuclear structure.

3. The next generation: SMC, E142, and E143

New data have recently become available from the SMC [10,11] experiment at CERN, and the E142 [12] and E143 [13] experiments at SLAC. These data include the first measurements on deuterons and ^{3}He, as well as significantly more precise proton data.

3.1. SMC

The first stage of the SMC experiment measured spin structure functions for deuterium [10]. The average energy of the incident muon beam was 100 GeV, polarized to 80%. The target was composed of deuterated butanol beads polarized using Dynamic Nuclear Polarization (DNP) to an average polarization of around 40%.

Target polarization reversal occurred about every eight hours. The kinematics covered were $0.006 < x < 0.60$ and $\langle Q^2 \rangle = 4.7$ (GeV/c)^2, and only $A_\parallel$ was measured.

The second stage of this experiment measured proton spin structure functions [11]. The average energy of the muon beam was increased to 190 GeV. The target material was butanol with an average polarization of 86%, and polarization reversals occurred every five hours. The kinematics covered were $0.003 < x < 0.70$ and $\langle Q^2 \rangle = 10$ (GeV/c)^2, and both $A_\parallel$ and $A_\perp$ [14] were measured.

The SMC data and the SLAC data are complimentary. The kinematic range covered by SMC is very good, but the statistics are limited. The SLAC experiments are limited in their kinematic coverage, but have very small statistics.

3.2. E142

E142 [12] measured neutron spin structure functions using an electron beam incident on a ^{3}He gas target. The energy of the incident beam ranged from 19.4–25.5 GeV, and had an average polarization of 39%. The beam helicity was randomly selected on a pulse-to-pulse basis. Polarization of the target occurred via spin-exchange with optically pumped rubidium vapor with the average polarization around 35%. The kinematics covered were $0.03 < x < 0.6$ and $\langle Q^2 \rangle = 2$ (GeV/c)^2, and both $A_\parallel$ and $A_\perp$ were measured.

3.3. E143

E143 [13] measured spin structure functions for the proton and deuteron with electron beam energies of 9.7, 16.2, and 29.1 GeV. Only the proton data at E=29.1 GeV are currently available. The average beam polarization was increased from that of E142 to 84% for this experiment. The targets used were $^{15}NH_3$ and $^{15}ND_3$, polarized via DNP to average polarizations of around 65% and 25%, respectively. The kinematics covered were $0.029 < x < 0.8$ and $\langle Q^2 \rangle = 3$ (GeV/c)^2, and both $A_\parallel$ and $A_\perp$ were measured.

3.4. Neutron/Deuteron Data Summary

The asymmetry and extracted xg_1 results for the SMC and E142 experiments are shown in Fig. 1. A world fit to all available proton spin structure function data was used to extract neutron asymmetries from the measured SMC deuterium results. These agree well with the E142 measured asymmetries. Table 1 shows a summary of the deuteron and neutron sum rule measurements and predictions. Consecutively, the rows in Table 1 show the average Q^2 of the measurements/calculations; the target type (d for deuterium and n for neutron); the strong coupling constant $\alpha_s(Q^2)$ at the Q^2 indicated; the Ellis-Jaffe sum rule prediction for the given target type

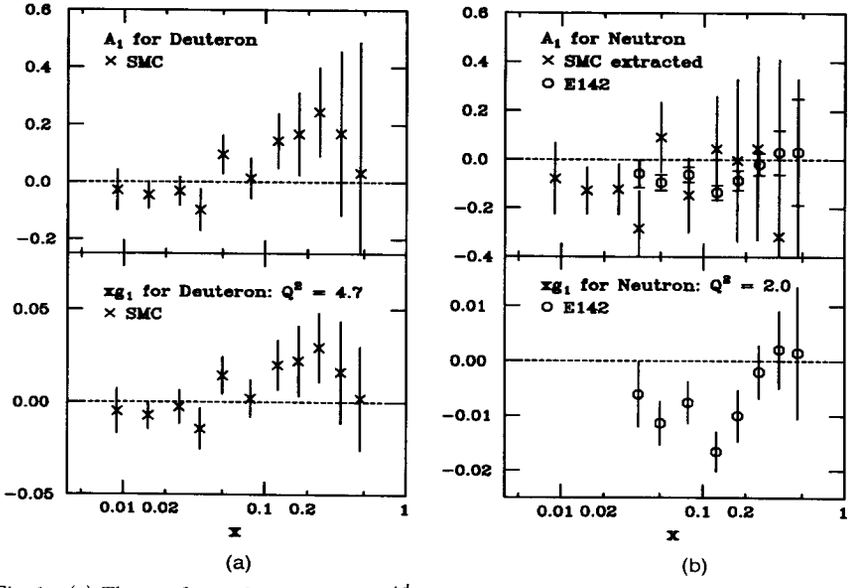

Fig. 1. (a) The top figure shows the SMC A_1^d results, and the bottom figure shows xg_1 for the SMC measurements evolved to a constant Q^2 of 4.7 (GeV/c)^2. (b) The top figure shows the E143 A_1^n results along with SMC results which were extracted from the deuterium data using a world fit to all available proton data. The bottom figure shows xg_1 for the E142 measurements evolved to a constant Q^2 of 2.0 (GeV/c)^2. All errors shown are statistical.

and Q^2; the experimental sum rule integral; the extracted quark helicity content variables, Δq and Δs; The Bjorken sum rule prediction for the given Q^2; and finally, the measured Bjorken integral. The errors on the sum rule predictions have been updated to include an uncertainty on neglected higher order QCD corrections. This error for the nonsinglet correction is assigned to be the estimated fourth-order correction [15]. Similarly, this error for the singlet correction is assigned to be the estimated third-order correction [16]. This uncertainty becomes significant for the low Q^2 predictions. The quantities Δq and Δs have been updated from the original published values to reflect improved QCD corrections. The Bjorken integral experimental results were obtained using E143 proton data evolved to the appropriate Q^2.

The first two columns of Table 1 show measured results at the average Q^2 of the indicated experiment. The third column shows the E142 results evolved to a Q^2 of 5 (GeV/c)^2. The Q^2 evolution was done in an approximate way, using the Q^2 dependence of the QCD corrections, the quark model interpretation of the nucleon, and a simple model for the Δs contribution. This model assumes that Δs varies

Table 1: Neutron/Deuteron sum rule summary.

	SMC	E142	E142
Q^2 (GeV/c)^2	5	2	5
Target	d	n	n
α_s	0.26 ± 0.04	0.40 ± 0.05	0.26 ± 0.04
EJ pred.	0.077 ± 0.004	-0.008 ± 0.007	-0.016 ± 0.005
Γ meas.	0.023 ± 0.025	-0.022 ± 0.011	-0.027 ± 0.014
Δq	0.10 ± 0.26	0.44 ± 0.12	0.47 ± 0.13
Δs	-0.16 ± 0.09	-0.05 ± 0.04	-0.04 ± 0.05
BJ pred.	0.185 ± 0.006	0.162 ± 0.012	0.185 ± 0.006
$\Gamma_p - \Gamma_n$ meas.	0.224 ± 0.059	0.146 ± 0.015	0.164 ± 0.018

sufficiently slowly with Q^2 such that it can be estimated using the world average value of -0.10 ± 0.03. The extracted value for Δs from the evolved data is consistent with the model assumptions.

As can be seen from the table, the results from SMC and E142 are consistent with each other, and both sets of data agree with the Bjorken sum rule prediction. The E142 result supports the Ellis-Jaffe prediction, while the SMC result does not. This has important consequences for the quark model interpretation. From the SMC result, a negative Δs is extracted which is inconsistent with zero, and a small Δq is also extracted; however, both of these quanties have large errors. The E142 data indicate a Δs which is consistent with zero and a large value of Δq compared to the SMC deuterium results and all proton results. Clearly, more data on deuterons and neutrons are needed to sort out this difference in interpretations.

3.5. Proton Data Summary

Recent proton results for g_1/F_1 are shown in Fig. 2. The E80 and EMC proton results were not included to avoid confusion on the plot, but all the proton data are in very good agreement. The E130 data were converted to g_1/F_1 assuming $A_\perp = 0$. For the large beam energies of the SMC experiment the expression $g_1/F_1 = A_1$ is valid, but this is only an approximation at the SLAC kinematics. Using the fits to $F_2^p(x, Q^2)$ [17] and $R(x, Q^2)$ [18] to evaluate $F_1(x, Q^2)$ at a fixed $Q^2 = 3.0$ (GeV/c)^2, the E143 data are evolved to a constant Q^2 assuming g_1/F_1 is independent of Q^2. These results are shown in Fig. 3. Table 2 shows a summary of the most recent (and precise) proton sum rule measurements and predictions. The rows in the table are defined as in Table 1. The experimental Bjorken integral results were evaluated using

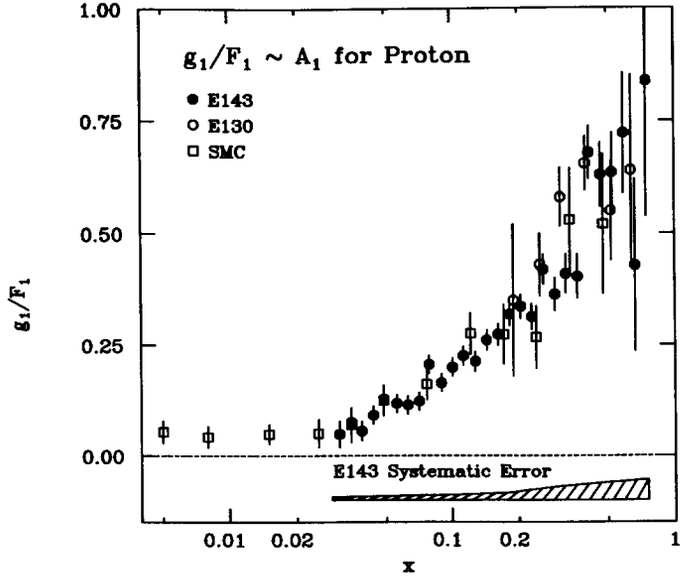

Fig. 2. Results for g_1/F_1 for the proton for experiments E143, E130, and SMC. Data from E80 and EMC have been left off the plot in order to see the most recent data clearly. All the proton data from all experiments are in good agreement. Errors include statistical only. The systematic error band is shown for the most precise measurements from E143.

Table 2: Proton sum rule summary.

	SMC	SMC	E143	E143
Q^2 (GeV/c)^2	10	5	3	5
α_s	0.23 ± 0.02	0.26 ± 0.04	0.35 ± 0.05	0.26 ± 0.04
EJ pred.	0.171 ± 0.004	0.169 ± 0.005	0.160 ± 0.006	0.169 ± 0.005
Γ meas.	0.136 ± 0.016	0.134 ± 0.016	0.129 ± 0.010	0.137 ± 0.011
Δq	0.25 ± 0.15	0.25 ± 0.15	0.29 ± 0.11	0.29 ± 0.11
Δs	-0.11 ± 0.05	-0.11 ± 0.05	-0.10 ± 0.04	-0.10 ± 0.04
BJ pred.	0.189 ± 0.003	0.185 ± 0.006	0.171 ± 0.010	0.185 ± 0.006
$\Gamma_p - \Gamma_n$ meas.	0.164 ± 0.022	0.161 ± 0.021	0.153 ± 0.016	0.164 ± 0.018

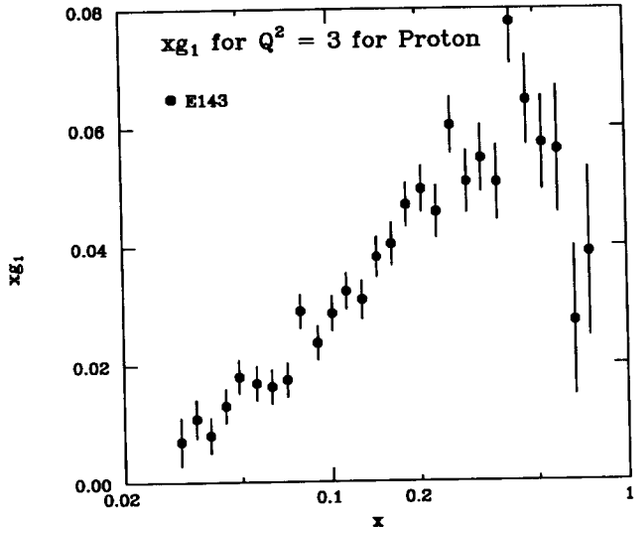

Fig. 3. The structure function g_1^p (scaled by x) from E143 is shown at a fixed Q^2=3.0 (GeV/c)^2. The errors are statistical only.

E142 data evolved to the appropriate Q^2. Columns 1 and 3 show the SMC and E143 results at the average experimental Q^2 values of 10 and 3 (GeV/c)^2, respectively. Columns 2 and 3 show the same results evolved to a constant $Q^2 = 5$ (GeV/c)^2.

The method of evolving was discussed in the neutron/deuteron results section. The two experiments agree very well, especially after being evolved to the same Q^2. The data are consistent with the Ellis-Jaffe sum rule being violated, but the Bjorken sum rule predictions are in good agreement with the data. The net quark helicity content Δq is small compared to the naive relativistic quark model expectation of 0.75. The strange quark helicity Δs is negative and inconsistent with zero.

A comparison of all the experimental results on extracted quark helicity content is shown in Fig. 4. These results are evolved to Q^2= 5 (GeV/c)^2. The agreement between experiments is good. It is important to note that when only first order QCD corrections are included and the data are not evolved to the same Q^2, the agreement between experiments is not nearly as good. Thus, it is very important to treat the data properly before different experiments can be compared to each other. An error-weighted average over all experiments of these results yields $\Delta s = -0.10 \pm 0.03$ and $\Delta q = 0.29 \pm 0.07$.

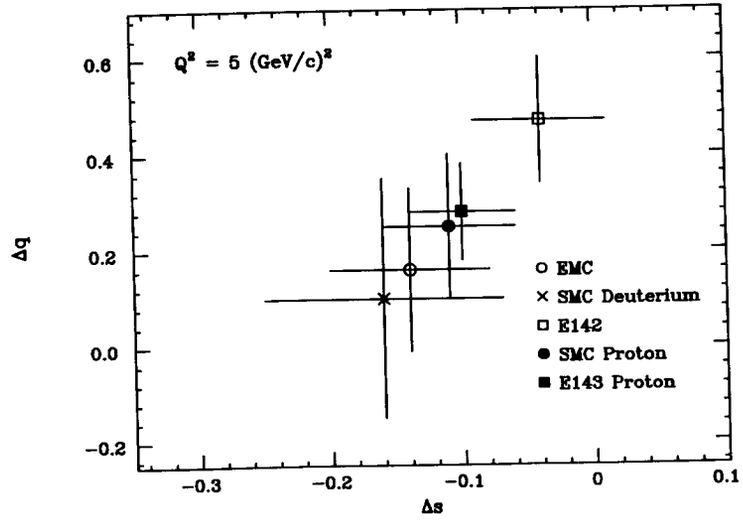

Fig. 4. The quark helicity content of the proton as extracted from various measurements is shown for Δq versus Δs. The data have been evolved to a constant $Q^2 = 5$ (GeV/c)^2, and include third order nonsinglet QCD corrections and second order singlet QCD corrections. All experiments are in reasonable agreement within errors.

4. Conclusions and Outlook

The spin structure function data support the Bjorken sum rule predictions, and thus an important test of QCD is passed; however, the Ellis-Jaffe sum rule predictions for the proton are violated. In the context of the quark model, this implies that a nonnegligible fraction of the proton helicity is carried by either strange quarks, gluons, or both. The last hope for the Ellis-Jaffe predictions may be found in the low-x extrapolation. The SMC proton data hint that $g_1^p(x)$ starts to rise at low x rather than remaining constant as extrapolations to zero have assumed. A confirmation of this result with improved precision could conceivably change our interpretation of the experimental results [19].

A number of experimental programs will produce new spin structure results in the future, and thus provide more stringent sum rule tests. Already measured E143 data on deuterium, transverse structure functions, and Q^2 dependent studies will be available soon. The SMC will take more data on both proton and deuteron targets,

which will be valuable for the low-x information. A new program at SLAC will begin in the fall of 1995 using a 50 GeV incident electron beam and new small-angle magnetic spectrometers. This program includes E154 [20] with a ^{3}He target and E155 [21] with $^{15}NH_3$ and $^{15}NH_3$ targets. Also, HERMES at HERA [22] is approved to measure spin-dependent structure functions of the proton and neutron starting in the fall of 1995. The data from these experiments will improve our understanding of the nucleon spin structure, and should answer many questions that have arisen due to current experimental results.

REFERENCES

1. J. D. Bjorken, Phys. Rev. **148**, 1467 (1966); Phys. Rev. **D1**, 1376 (1970).
2. Particle Data Group, Phys. Rev. **D45**, S1 (1992).
3. S. A. Larin and J. A. M. Vermaseren, Phys. Lett. **B259**, 345 (1991) and references therein.
4. J. Ellis and. R. Jaffe, Phys. Rev. **D 9**, 1444 (1974); Phys. Rev. **D10**, 1669 (1974).
5. S. A. Larin, CERN-TH-7208/94 (modified), to be published in Phys. Lett.
6. F. E. Close and R. G. Roberts, Phys. Lett. **B316**, 165 (1993).
7. M. Alguard et al., SLAC E80, Phys. Rev. Lett. **37**, 1261 (1976); Phys. Rev. Lett. **41**, 70 (1978).
8. G. Baum et al., SLAC E130, Phys. Rev. Lett. **51**, 1135 (1983).
9. J. Ashman et al., EMC, Nucl. Phys. **B328**, 1 (1989).
10. B. Adeva et al., SMC, Phys. Lett. **B302**, 533 (1993).
11. D. Adams et al., SMC, Phys. Lett. **B329**, 399 (1994).
12. P. L. Anthony et al., E142, Phys. Rev. Lett. **71**, 959 (1993).
13. K.Abe et al., E143, SLAC–PUB–6508 (1994), submitted to Phys. Rev. Lett.
14. D. Adams et al., SMC, CERN–PPE–94–116 (1994), subm. to Phys. Lett. B.
15. A. Kataev and V. Starshenko, CERN–TH 7198/94.
16. A. Kataev, CERN–TH 7333/94.
17. NMC, P. Amaudruz et al., Phys. Lett. **B295**, 159 (1992).
18. L. W. Whitlow et al., Phys. Lett. **B250**, 193 (1990).
19. F. E. Close and R. G. Roberts, RAL–94–071 (1994).
20. R. Arnold et al., SLAC proposal E154 (1993).
21. R. Arnold et al., SLAC proposal E155 (1994).
22. K. Coulter et al., HERMES proposal DESY/PRC 90–1 (1990).